Postprint of: Deja M., Lichtschlag L., Uhlmann E., Thermal and technological aspects of double face grinding of C45 carbon steel, Journal of Manufacturing Processes, Vol. 64 (2021), pp. 1036-1046, DOI: 10.1016/j.jmapro.2021.02.023

Thermal and technological aspects of double face grinding of C45 carbon steel

AUTHORS

Mariusz Deja[1]*, Linus Lichtschlag[2], Eckart Uhlmann[2]

AFFILIATION

[1]Faculty of Mechanical Engineering, Department of Manufacturing and Production Engineering, Gdańsk University of Technology, Gabriela Narutowicza Street 11/12, 80 - 233 Gdańsk, Poland

[2]Chair of Machine Tools and Manufacturing Technology, Institute for Machine Tools and Factory Management, Technische Universität Berlin, Pascalstraße 8 - 9, 10587 Berlin, Germany

***Corresponding Author**, Phone: +48 58 347 29 67, Mail: mariusz.deja@pg.edu.pl

Mariusz Deja: orcid.org/0000-0002-1874-9015

ABSTRACT

In grinding, the contact zone temperature is a decisive factor influencing the achievable surface quality and the grinding tool wear. In contrast to other grinding processes, only few information regarding double face grinding with planetary kinematics when processing steel is known up to date. Since the successive substitution of industrial double-sided lapping processes by double-sided grinding, it has become necessary to the conducted research in order to provide deeper understanding of the process and factors that influence it. To determine the workpiece temperature during grinding of C45 components, silicon temperature sensors were integrated into the workpiece holders and technological investigations were carried out. The influences and interactions of the mean cutting speed, cooling lubricant flow rate and cutting ability of the grinding wheels on the resulting workpiece temperature were analysed. Subsequently, modelling enabled an empirical estimation of the resulting workpiece temperature for processes in the investigated test area. With regard to the design and optimization of processes for machining plane-parallel workpiece surfaces, this model is a helpful tool for avoiding thermally induced workpiece damage and reduction of tool wear. Furthermore, the method can be used

to conduct further examinations on the grinding process and to reduce the amount of cooling lubricant used, to improve life cycle assessment.

KEYWORDS

Grinding; Temperature Measurement; Abrasive Finishing; Empirical Modeling; Manufacturing Process

HIGHLIGHTS

- Development of a method for measuring workpiece temperature in double face grinding with planetary kinematics
- Investigation of the influence of the mean cutting speed, tools' cutting performance and coolant flow on the workpiece temperature
- Determination of an empirical model to predict the temperature of a steel workpiece during processing time

1. INTRODUCTION

The machining process of double face grinding with planetary kinematics is used for machining plane-parallel workpiece surfaces such as those of metallic bearings and piston rings as well as ceramic sealing discs and wafers. The double-sided batch wise machining of the workpieces is characteristic for the machining process. The kinematics and arrangement of the tools are similar to the double face plane-lapping from which the manufacturing process originated. In contrast to this, double face grinding is carried out using bonded abrasive and cooling lubricant. The machine structure consists of two horizontally arranged grinding wheels, between which the unclamped workpieces are placed in circular, externally toothed workpiece holders, Figure 1. These workpiece holders are guided by a driven inner pin ring and usually stationary outer pin ring. During machining, the workpieces perform cycloidal movements in relation to the grinding wheels. These movements result from the superimposition of the driven grinding wheels, the rotational movements of the inner pin ring and the resulting workpiece holder rotation. The work result on the workpieces shows a high degree of plane-parallelism of the machined surfaces. The tool marks on the workpieces have an undefined curved, overlapping characteristic. The advantages of double face grinding with planetary kinematics are the tension-free holding of the workpieces in the holders and evenly distributed load of the workpiece surfaces while grinding [1-4].

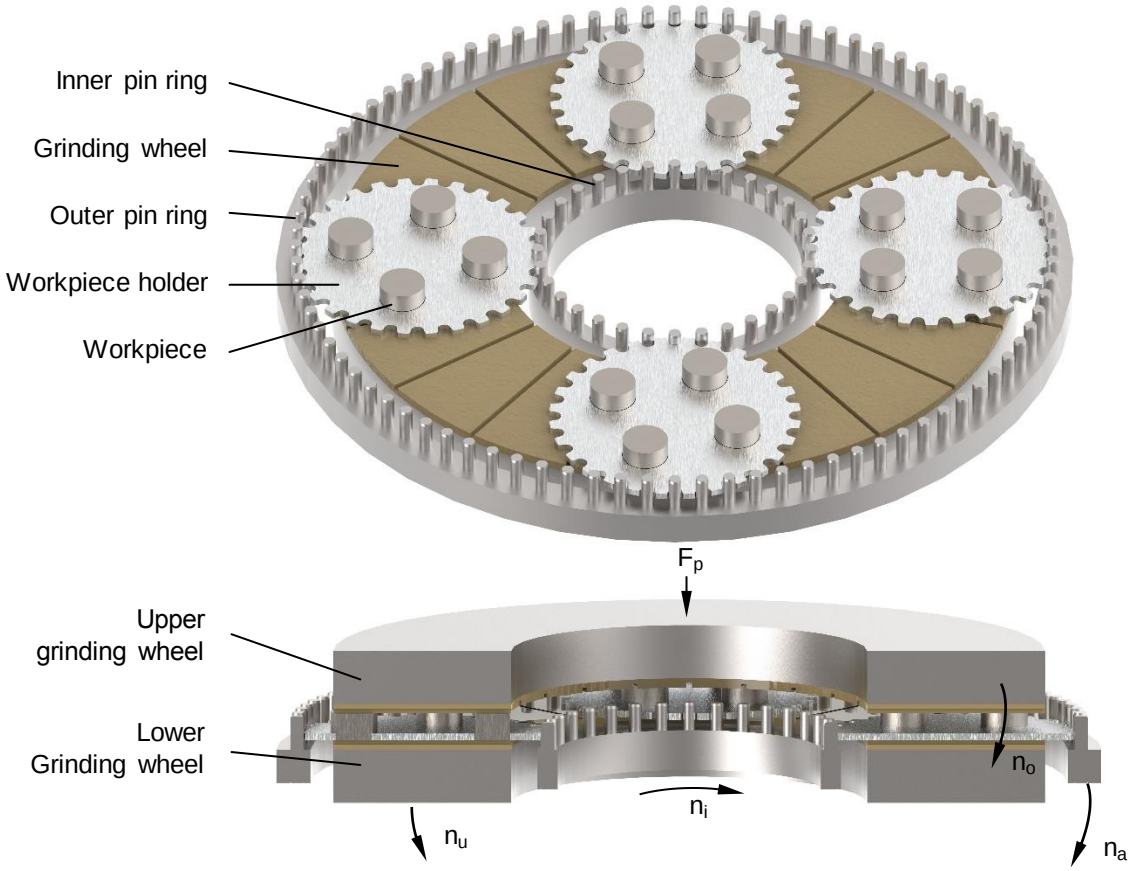

Rotational speed lower grinding wheel	n_u
Rotational speed upper grinding wheel	n_o
Rotational speed inner pin ring	n_i
Rotational speed outer pin ring	n_a
Process force	F_p

Figure 1: Main components of the machine system for double face grinding with planetary kinematics [8]

The advantage over double face plane-lapping is also a lower environmental impact due to the substitution of the lapping emulsion by bonded grains in the grinding wheel and the use of a coolant circuit. Previous lapping processes can be replaced by grinding processes and achieve the same or better results in terms of productivity and quality [5, 6]. For the processing of sapphire, WANG ET AL. [7] showed that the productivity and achievable surface quality varies with the crystal orientation of the wafers used. Analyses of wear characteristics, process efficiency and possibilities for their reduction were carried out by UHLMANN ET AL. [8-10]. On this basis, LIST [11] developed an algorithm for the targeted selection of abrasive layers adapted on the specific production process. LICHTSCHLAG ET AL. [12, 13] conducted examinations to optimize the dressing processes, which had previously been based on practical knowledge. With the use of a developed measuring device to

determine profile wear, they found the profiling result as a function of the investigated dressing parameters. The selected cycloidal path shape of the dressers and the machined height of the dresser are decisive for generating the required grinding wheel flatness. Although the temperature in the working zone between the workpiece and the grinding wheel and, thus, the thermal energy transferred to the working partners is a process characteristic that must be considered, it has so far only been studied marginally compared to other grinding processes. However, since higher cutting speeds and working pressures can be achieved by substituting lapping with grinding, the thermal energy introduced into the system also increases.

This paper presents a method of measuring the temperature of steel workpieces in double face grinding. The proposed method is relatively simple and cheap allowing to collect reliable data from the physical environment of an advanced technological machining system characterised by simultaneous processing of two coplanar work surfaces using planetary kinematics. Section 2 of the paper contains a review of research performed in the area of thermal aspects of abrasive processes. Particularly, models based on the contact mechanics and used to estimate the temperature rise of the work surface in processes similar to double face grinding, i.e., in polishing, lapping and superfinishing, are analyzed. On the basis of this analysis, the general trends in measured temperatures during double face grinding experiments are anticipated. Section 3 gives the details of the developed research methodology for the temperature measurements using full-featured digital loggers with a silicon temperature sensor. Section 4 presents the results from grinding experiments showing the influence of a gradual decrease in the grinding efficiency (due to the wear of the grinding wheel) on the workpiece temperature, under constant technological parameters. Finally, the authors' contributions are summarised and further research directions are formulated in Section 5.

2. Thermal analyses of abrasive processes

Description of the complicated microscopic interactions between grains and workpiece material in their contact zone poses a crucial problem of modelling the abrasive processes. Thermal analyses of grinding, lapping, polishing or superfinishing are mostly based upon the application of moving heat source theory [14]. The grinding zone is modelled as a source of heat which moves along the surface of the workpiece.

The value of the heat flux is the frictional heat generated per unit time divided by the real area of tool-workpiece contact. Rectangular, triangular or parabolic shapes of the heat flux profile transferred into workpiece are usually assumed in the models for the simulations of temperatures or thermal stresses due to grinding [15, 16]. Jiang et al. [17] assumed a quadratic polynomial curve for describing the profile of the heat flux transferred into workpiece, giving more precise prediction ability on grinding forces and grinding temperatures. The energy partition to the workpiece is a critical parameter needed for calculating the temperature response and it can vary significantly depending on the type of the process, the tool and workpiece materials, fluid application and the operating conditions. The energy partition can be estimated from measurements of the workpiece temperature rise and grinding power consumption. It can also be obtained by matching measured workpiece temperatures to analytically calculated values [18, 19, 20]. The energy partition ε refers to the value for which the measured temperature response most closely matches the temperature computed from the thermal model. With the inverse heat transfer method, the heat flux to the workpiece surface is calculated form the measured temperature distribution within the workpiece [14, 21].

Double face grinding is characterized by two-body machining interactions as in the case of conventional grinding or superfinishing, and furthermore, by full workpiece-tool contact during machining as in lapping (full workpiece area) or superfinishing (full tool area). BULSARA ET AL. [22] developed a model based on the contact mechanics to estimate the temperature rise of the work surface in polishing and lapping – Figure 2 a. In this model, the normal force $F_{n,i}$ acting on the *i*-th abrasive particle is derived from a mechanistic analysis of abrasive-workpiece contact – Figure 2 b. At the microscopic level, the mechanical action of an abrasive is considered as the repeated application of a sharp and conical sliding indenter to the work surface. Assuming that the lap is perfectly rigid and non-deformable body, and that all abrasive particles are conical indenters with the geometry presented in Figure 2 b, the normal force $F_{n,i}$ acting on the *i*-th abrasive particle having a mean diameter (size) x_i, for a fully developed plastic contact, is given by:

$$F_{n,i} = \pi H \tan^2 \theta (x_i - X)^2, \tag{1}$$

where: H is the mean contact pressure equaled to workpiece hardness, θ is a semi-apical angle of a conical sliding indenter, $(x_i - X)$ is the depth of penetration of the i-th particle having a mean size (diameter) x_i greater than the separation distance X into the work surface.

a)

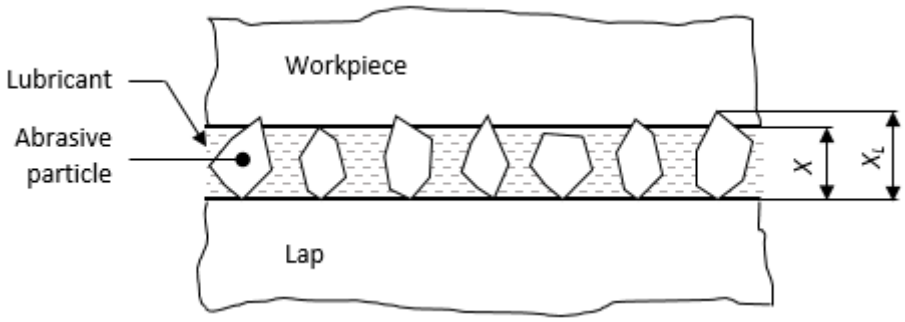

b)

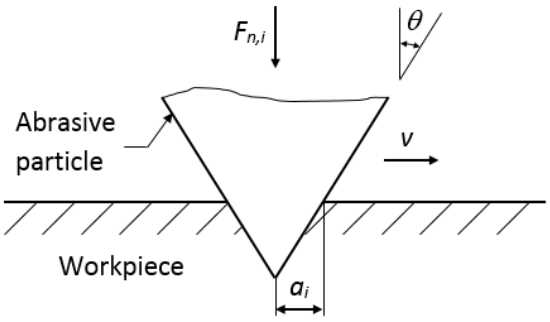

Figure 2. Schematic drawing of abrasive-workpiece contact during lapping (a) with a mechanical model of the contact between an abrasive particle and the workpiece (b); based on [22]

The sum of the individual normal forces $F_{n,i}$ on the cutting edges is equal to the total normal force $F_{n,\text{total}}$ which can be approximated as:

$$F_{n,total} = \pi NH \tan^2\theta \int_x^{X_L} (x - X)^2 \varphi(x) dx, \quad (2)$$

where: X_L is the size of the largest particle in the abrasive slurry, N is the total number of particles between the workpiece and the lap, x is the size (mean diameter) of abrasive particles described by a probability density function $\varphi(x)$.

A developed mechanical model was combined in [22] with Jaeger's theory of moving sources of heat [23] and Blok's theory of heat partition [24] to estimate the local temperature rise at abrasive-workpiece

contacts. The action of an active abrasive particle was modeled as a heat source moving over the surface of a semi-infinite solid, i.e., workpiece, with velocity *v*. The heat generated at the contact between an active particle and the workpiece is taken as the product of the friction force F_i on the *i*-th particle and the relative sliding velocity *v* between the particle and the work surface. The generated heat flux q_i, assumed to be uniformly distributed over the projected area of this contact, can be written as:

$$q_i = \frac{F_i v_i}{\pi {a_i}^2} = \frac{\mu F_{n,i} v}{\pi {a_i}^2}\,, \tag{3}$$

where: μ is the coefficient of friction and *v* is the relative sliding velocity of an abrasive particle, a_i is the radius of the projected circle of the contact assumed to resemble a fully plastic indentation produced by the action of a conical indenter on the work surface.

Using the method of energy partition proposed by BLOK [24] and assuming that all of the generated heat flows either into the workpiece or the abrasive with no loss to the surroundings, the following equation was derived to calculate the individual contact temperature rise:

$$T_i = \frac{1.22\mu v\sqrt{F_{n,i}H}}{\sqrt{\pi}} \frac{1}{K_W\sqrt{\pi(0.6575+P_c)+\frac{3.66\pi K_A}{8}}} \tag{4}$$

where: K_W, K_A are the coefficients of the thermal conductivity of the work material and abrasive respectively, P_c – is the workpiece Peclet number.

As shown in [25, 26, 27, 28], the model developed in [22] is relevant to a variety of abrasive finishing processes with machining interactions considered as a combination of two-body and three-body wear, i.e., lapping or polishing. This model was also successfully adopted by CHANG ET AL. [29] to estimate the resulting surface roughness of the superfinishing, which is an example of a process with two-body machining interactions – Figure 3.

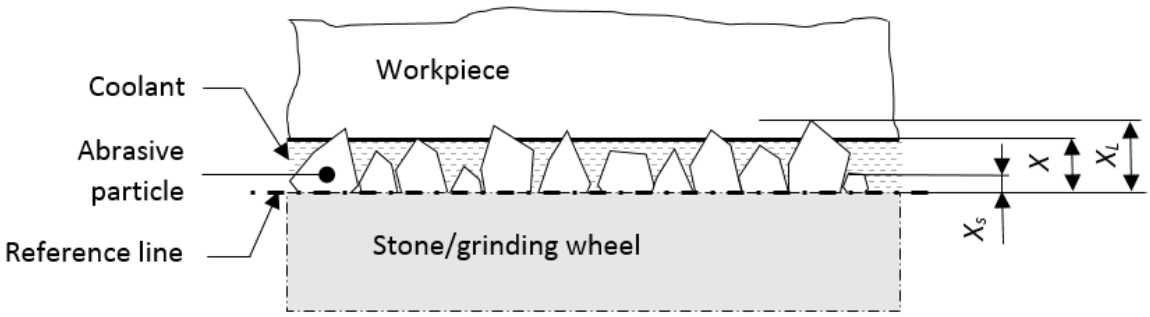

Figure 3: Tool-workpiece contact in superfinishing or in double face grinding in lapping configuration; based on [29]

Its application to superfinishing process required the information about how the abrasive cutting edges and their protrusion heights are distributed at and near the stone surface, as the number of particles actively engaged in material removal depends, among other parameters, on the applied normal force. In this model the work surface and the tool surface reference line are separated by a distance X, as shown in Figure 3. The cutting edges on the stone surface are statistically distributed between the smallest value, X_s, and the largest value, X_L. To measure height distribution, the surface topography of a 600 grit aluminum oxide stone used for superfinishing was quantitatively described using scanning phase-shift interferometer. Two statistical probability functions, bounded normal and bounded three-parameter lognormal distributions were selected to fit the cutting edges height distribution. The latter distribution was found to provide a more accurate representation of cutting edge height distribution. The predicted surface roughness was in good agreement with experimental results and the process appeared to be self-dressing as the active tool surface characteristics was nearly constant throughout stone life.

In the tests presented in this article, the wheel wear was not investigated in detail as the focus was on the measurement of the workpiece temperature. Moreover, the influence of a gradual decrease in the grinding efficiency (due to the wear of the grinding wheel) on the workpiece temperature, at the constant cutting speed, was also analyzed. Conducted experiments allowed to develop empirical models of temperature rises under given technological parameters and initial thermal conditions such as the workpiece and lubricant temperatures. One of the coefficients in the proposed nonlinear regression model can be assumed as an upper boundary of the workpiece temperature rise that can occur during double face grinding. The analysed process of double face grinding is undoubtedly more advanced to

perform and model than conventional grinding. Due to the complexity of double face grinding characterised by simultaneous processing of two coplanar work surfaces using planetary kinematics and intensive cooling, the empirical models seem to be effective to use in industrial practice. BRINKSMEIER ET AL. [30] pointed out that the field of possible applications for empirical models using regression analysis is vast and still expanding, especially for special applications and such a task is certainly the process under analysis. Nevertheless, further research will focus on adopting the models developed for lapping and superfinishing as they appear applicable to predict an upper boundary of the average contact temperature in double face grinding, since heat loss into the abrasive slurry has been neglected in [22]. Following CHANG ET AL. [29] a cutting edge height distribution and the wheel wear will have to be determined. Due to large sizes of tools used in double face grinding the cutting edge heights and the wheel wear can be measured by profiling or microscopic observation of elastomeric impressions made to accurately record detail on the active surface of the tool. The determination of the energy partition to the workpiece, both grinding wheels and lubricant, will be the final step in modelling the grinding temperature. The applicable method for the temperature measurements is the key issue for performing the energy partition, regardless of the partitioning method used for modelling. So far, the temperature measurements of steel workpieces grinded in the machining system under consideration has not been described in the literature.

Although the microscopic interactions between grains and workpiece material in the grinding contact zone were not considered in the empirical model presented in this paper, the wear assessment by microscopic observations of other grinding wheels [31, 32] supported by the models developed in [22] made it possible to anticipate general trends in measured temperatures during performed grinding experiments. Thus, the wheel wear by blunting of abrasive grains and filling the pores of the grinding wheels with the machining chips gradually reduces the grinding efficiency. This typically results in an increased number of active grains and lower heights of cutting edges. If the number of the cutting edges increases, the contact forces decrease and, according to Equation 4, the values of individual temperature rises should be lower under unchanged process parameters and for the same mechanical properties of the work material and abrasive. Tool conditioning restored the abrasive properties which again resulted in higher values of workpiece temperature. These tendencies were observed during all tests presented in

this article. In addition, due to the higher thermal conductivity of metallic materials compared to ceramic materials, it can be assumed that the heat dissipation via chips, cooling lubricant, grinding wheel and workpieces will shift to the advantage of the workpieces. A lower workpiece temperature and thermal load will result. It is known from other grinding processes that this has a considerable influence on the achievable surface quality. In particular, grinding burn and thermally induced changes in the edge zone must be avoided [33, 34].

Initial investigations to determine the grinding temperature during double face grinding with planetary kinematics were carried out only by DEJA ET AL. [35]. Using a measuring system integrated in workpiece holders, they measured the workpiece temperature prevailing during Al_2O_3 machining. The results led to a model to describe the change in workpiece temperature as a function of selected process parameters. However, it is unknown to what extent the knowledge gained can be transferred to the machining of metallic materials.

3. EXPERIMENTAL SETUP AND INVESTIGATIONS

The experiments were carried out on a prototype machine tool for high speed double face grinding with planetary kinematics, developed at the Institute for Machine Tools and Factory Management (Institut für Werkzeugmaschinen und Fabrikbetrieb - IWF), Technische Universität Berlin, Germany, in cooperation with the machine tool manufacturer Stähli AG, Pieterlen/Biel, Switzerland. The design of this unique machine tool allows for performing high-productivity grinding, resulting in higher removal rates $\Delta\dot{h}_w$ and shorter processing time t_p [36]. The cooling lubricant is supplied via 40 through holes with a diameter of d_h = 4 mm distributed on two rings (ϕ330 and ϕ462) in the upper grinding wheel, Figure 4.

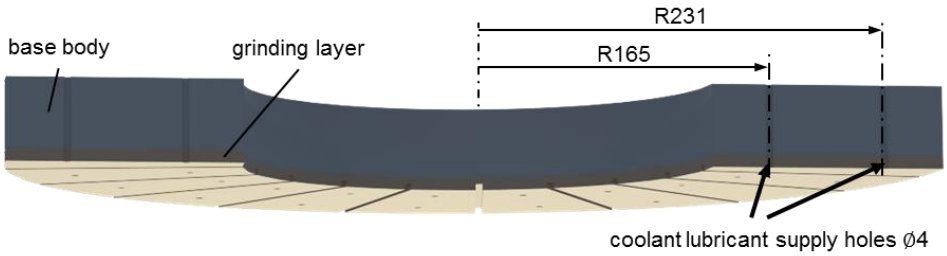

Figure 4: Upper grinding wheel with through-holes for the cooling lubricant supply

To achieve high values of cutting speeds and unit pressures, recommended for machining e.g. brittle hard materials, grinding wheels can rotate at the speed up to 2000 rpm with the load applied to

workpieces up to 4000 daN. This is a fourfold increase compared to conventional double face grinding machines with planetary kinematics. Mean cutting speeds $\bar{v}_c$ of up to 45 m/s can be achieved when a maximal rotational speed of the inner pin ring is 1000 rpm. Due to the mass and size of rotating tools with an outer radius r_o = 265 mm, the machine tool system used for experiments is characterised by a highly rigid portal design. This allows processing with high grinding wheel speeds as well as high grinding forces and torques. In addition, changeable kinematical conditions with the radius dependent velocity and acceleration distribution affect the non-uniform profile wear of grinding wheels, in single [37-40] or double face [41] lapping alike, as well as in grinding with lapping kinematics [8, 9, 10, 42]. Previous experiments performed on Al_2O_3 workpieces allowed the determination of an empirical model to predict the change in workpiece temperature during double face grinding [35]. Similarly, as in aforementioned studies, full-featured digital temperature loggers were used to measure the temperature in the workpieces made of C45 carbon steel in the analysed machining system. The loggers saved the temperature data of the workpieces while they were being grinded. The iButton® temperature loggers of two types DS1922L [43] and DS1922E [44] made by IBUTTONLINK, LLC, Whitewater, Wisconsin, USA, were used. A DS1922L logger is characterised by the operating temperature range from – 40 °C to + 85 °C, a resolution of 0.0625 °C, a temperature accuracy of ± 0.5 °C and a minimum sampling frequency of 1 Hz. It was effectively used to measure the temperature of the ceramic workpieces within its operating range. The temperatures up to 60 °C recorded during experiments, were 25 °C lower than the upper range limit [35]. Lower temperatures were expected during grinding of workpieces made of C45 carbon steel because of the higher thermal conductivity of steel materials (k_{C45} = 43 W/m/K) comparing to the thermal conductivity of Al_2O_3 ceramics (k_{Al2O3} = 27 W/m/K). Nevertheless, the high-temperature logger DS1922E was used in addition to the low-temperature logger DS1922L to ensure that the maximum workpiece temperature is recorded accurately and not missed. The measuring range of the DS1922E sensor is between +15 °C and +140 °C. The temperature measurement setup was the same for DS1922L and DS1922E loggers which were placed independently in the workpieces, Figure 5.

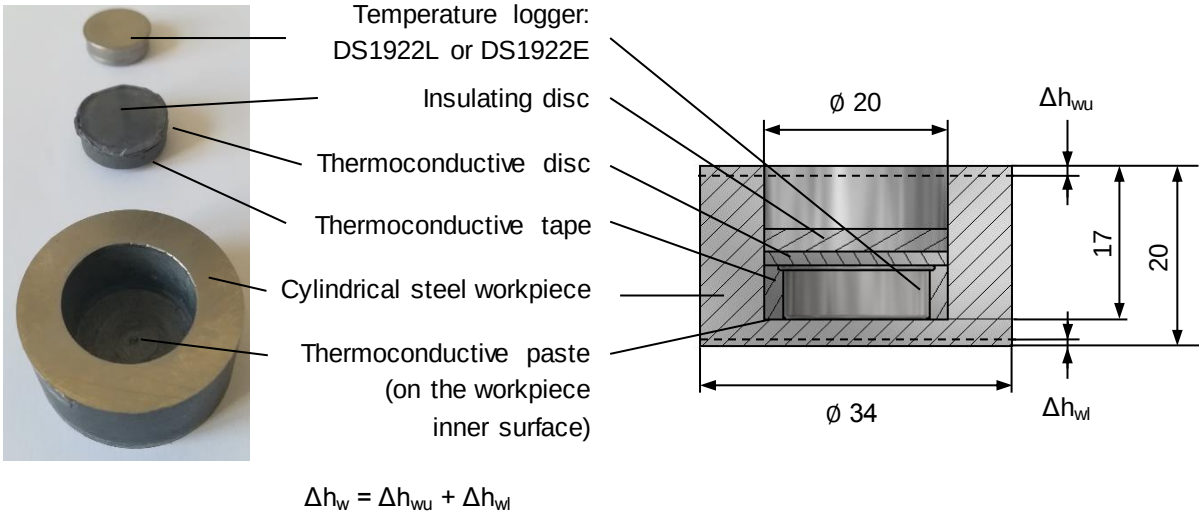

Figure 5: Measurement setup of a temperature logger in a workpiece

The standard uncertainty of the measurements after the calibration of selected temperature loggers was 0.13 K. The logger, covered with a thermoconductive disc and tape, was integrated in a steel workpiece. The generated heat was transmitted to the logger through the workpiece using thermoconductive elements. The coolant insulating disc was placed on the thermoconductive disc to protect a silicon sensor from the coolant even though the durable stainless-steel package is highly resistant to environmental hazards such as dirt, moisture and shock. A total of 4096 16-bit readings taken at a minimum sampling rate of 1 s and at equidistant intervals can be stored during experiments in a protected memory section. Data recording can be programmed to begin immediately, after a temperature alarm or after a user-defined delay. In this case, a delay of approximately 30 minutes was necessary in order to mount loggers in workpieces, place workpieces in carriers, set working parameters and stabilise the temperature. Temperature loggers communicate with a host computing device through the serial 1-wire protocol, which requires only a single data lead and a ground return. Temperature data can be read-out at any time after completing the experiments.

One measuring device with a programmed and installed temperature logger (DS1922L or DS1922E) as well as four cylindrical workpieces were placed in a single workpiece holder to measure the workpiece temperature while grinding, Figure 6. Therefore, five loggers (three DS1922L and two DS1922E) were placed in the five workpiece holders during each grinding process.

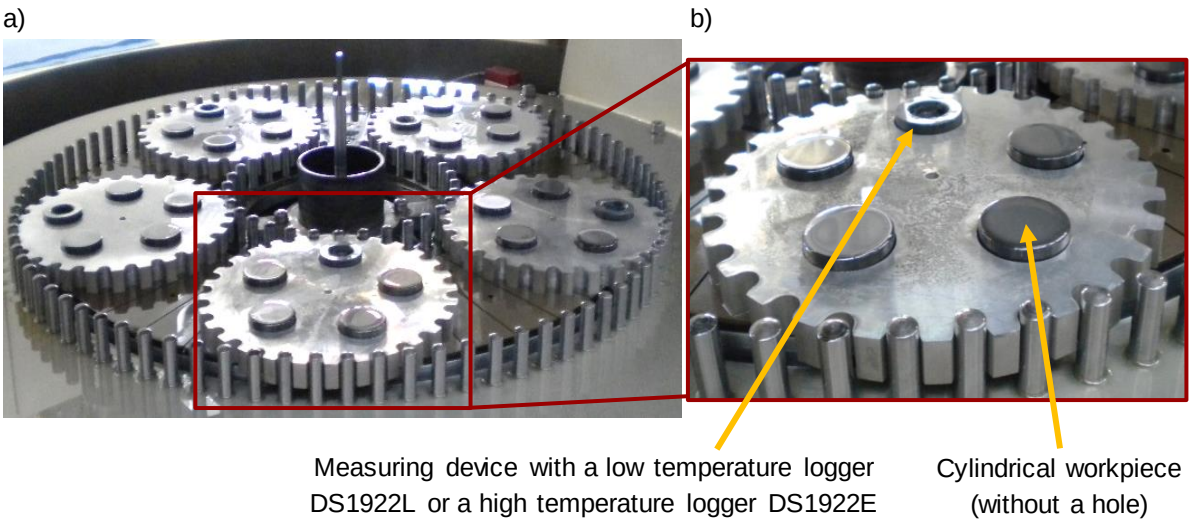

Figure 6: Arrangement of steel workpieces in a machining system for double face grinding with planetary kinematics: a) general view, b) single workpiece holder with a measuring device and four cylindrical workpieces

The main aim of the experiments was to examine the influence of the mean cutting speed $\bar{v}_c$ on the temperature of steel workpieces. Since the material removal rate $\Delta\dot{h}_w$ decreases while grinding due to tool wear, a conditioning process was carried out periodically to restore the cutting performance of the grinding tool. The grinding parameters of the performed experiments are presented in Table 1. The lowest coolant flow rate $\dot{Q}_{lub}$ = 20 l/min was applied only for the lowest average cutting speed $\bar{v}_c$ = 5 m/s. For higher speeds: $\bar{v}_c$ = 10 m/s and $\bar{v}_c$ = 15 m/s, more intensive cooling with the flow rate rate $\dot{Q}_{lub}$ = 40 l/min was used. Other parameters were not varied during the experiments.

Table 1: Grinding conditions during experiments

Grinding wheels		
Outer tool radius r_o	mm	265
Inner tool radius r_i	mm	132.5
Grain material		Cubic boron nitride (CBN)
Grain size d_g	-	D64
Abrasive grain concentration		C75
Bond type		Synthetic resin
Grinding parameters		
Mean cutting speed $\bar{v}_c$	m/s	5 10 15
Grinding pressure p_p	N/mm^2	0.11
Tool allocation B	%	11.53
Maximum depth of material removed per batch Δh_w	mm	3
Coolant flow rate $\dot{Q}_{lub}$	l/min	20 ($\bar{v}_c$ = 5 m/s) 40 ($\bar{v}_c$ = 10 m/s; 15 m/s)
Workpiece properties		
Material		C45
Hardness – Rockwell scale	HRC	45 ± 1
Diameter d_w	mm	34
Initial height h_{w0}	mm	20

The workpiece dimensions allowed a maximum workpiece height reduction of Δh_w = 6 mm evenly distributed to the top and bottom of the workpiece, with material removal of Δh_{wu} = 3 mm from the top and Δh_{wl} = 3 mm from the bottom, Figure 5. During grinding of ceramics, the workpiece height reduction was Δh_w = 4.8 mm resulting in the final height of the sample 15.2 mm and uniform material removal from the top and bottom of the workpiece [35]. During grinding of steel, the maximum depth of material removed per batch was Δh_w = 3 mm, due to the longer processing time obtained for smaller CBN grains – Figure 7. Further machining would overwrite the temperature data with a total of 4096 data entries. For the equidistant interval of 1 s (sampling frequency 1 Hz), the new temperature data can be stored within 4096 seconds. The overwriting was observed for one logger, although the temperature data recorded during processing was not deleted – Figure 7. The final height of the steel sample was 17 mm and the value of the final distance between sensor and the workpiece bottom outer face was 1.5 mm. The monitored temperature signals were not exactly equal to the contact temperature due to the

cooling and heat loss. In addition, the distance between the thermal sensor and workpiece bottom surface caused a brief delay in reflection of the contact temperatures. Following [45] and neglecting heat loss, the characteristic delay time for a thermal signal on one side to reach the other side can be calculated using the formula:

$$t_d = \frac{h^2}{D}, \tag{5}$$

where: h is the distance between the thermal sensor and workpiece bottom surface, D is a thermal diffusivity.

The delay in the measurement caused by the thermal penetration time decreases during grinding due to the material removal reducing the distance between the thermal sensor and workpiece bottom surface. For the initial distance h = 3 mm and assuming a thermal diffusivity D = 16 mm^2/s, the calculated delay time is about 0.56 s. For the final distance h = 1.5 mm obtained after removing the height of the material Δh_{wl} = 1.5 mm from the workpiece bottom surface, the calculated delay is 0.14 s. The delay time was not included during the measurements and further analyses as it was shorter than the interval of 1 s between the measurements (sampling frequency 1 Hz). Nevertheless, this effect can be compensated by calculating the time delay for the initial and current heights due to the material removals. The difference in the time delay Δt_d at the beginning and at the end of the process can be calculated using the equation:

$$\Delta t_d = \frac{\Delta h_{wl}(2h_i - \Delta h_{wl})}{D}, \tag{6}$$

where: h_i is the initial distance between the thermal sensor and workpiece bottom surface, Δh_{wl} is the height of the material removed from the bottom of the workpiece during grinding.

Figure 7 illustrates the measured temperature data determined for the grinding process with the parameters $\bar{v}_c$ = 5 m/s and $\dot{Q}_{lub}$ = 20 l/min, without taking into account the delay in the measurement caused by the thermal penetration time.

Process
Double face grinding with planetary kinematics

Machine tool
Stähli DLM 505 HS

Workpiece

Type	Test workpiece, cylindrical
Material	C45
Radius	r = 17.5 mm

Temperature stabilization	①	Removing loggers from workpieces	③
Inspection of a measuring sample	②	Temperature overwriting	④

Process parameter

Allocation	B	=	11.53	%
Mean cutting speed	$\bar{v}_c$	=	5	m/s
Coolant lubricant	Rhenus GP5			
Volume flow	$\dot{Q}_{lub}$	=	20	l/min
Temperature	T_{lub}	=	21.7	°C

Tool

Type	B64 C75			
Grain material	CBN			
Bonding type	Synthetic resin			
Grain size	d_g	=	D64	
Grain concentration	C	=	3.3	ct/cm³
Outer radius	r_o	=	265	mm
Inner radius	r_i	=	132.5	mm

Logger 1
Logger 2
Logger 3
Logger 4
Logger 5

t_{bi} time at the beginning of experiment E_i
t_{ei} time at the end of experiment E_i
t_{maxi} time when maximum temperature in experiment E_i was reached

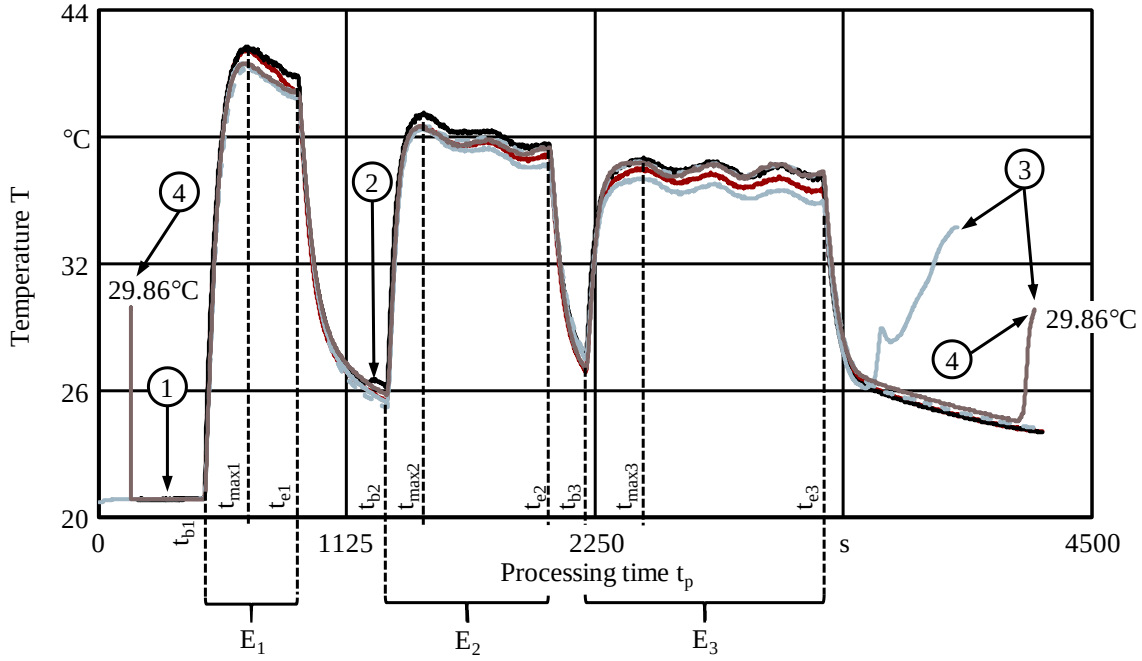

Figure 7: Workpiece temperatures recorded by loggers during three experiments on C45

During all three experiments E_1, E_2 and E_3 a height of $\Delta h_w = 1$ mm was removed. Decreases of the material removal rate $\Delta \dot{h}_w$ caused by the tool wear extended the processing time while the mean cutting speed $\bar{v}_c$ remained constant. However, the workpiece temperature decreased. In all experiments, intensive cooling and reduced cutting performance of the tools caused a decreasing workpiece temperature after reaching the maximum value, Figure 7.

The temperature was recorded once every second and the mean values of the workpiece temperatures during the entire processing time were used for modelling the temperature increase. In the analysed example with $\bar{v}_c$ = 5 m/s, the maximum temperature reached before the end of the machining operation in the experiments E_1, E_2 and E_3 ($t_{maxi} < t_{ei}$, for i = 1, 2, 3), is marked on the chart by the ◊ symbol, Figure 8.

Process
Double face grinding with planetary kinematics

Machine tool
Stähli DLM 505 HS

Workpiece

Type	Test workpiece, cylindrical			
Material	C45			
Radius	r	=	17.5	mm

Process parameter

Allocation	B	=	11.53	%
Cutting speed	$\bar{v}_c$	=	5	m/s
Coolant lubricant	Rhenus GP5			
Volume flow	$\dot{Q}_{lub}$	=	20	l/min
Temperature	T_{lub}	=	21.7	°C

Tool

Type	B64 C75			
Grain material	CBN			
Bonding type	Synthetic resin			
Grain size	d_g	=	D64	
Grain concentration	C	=	3.3	ct/cm³
Outer radius	r_o	=	265	mm
Inner radius	r_i	=	132.5	mm

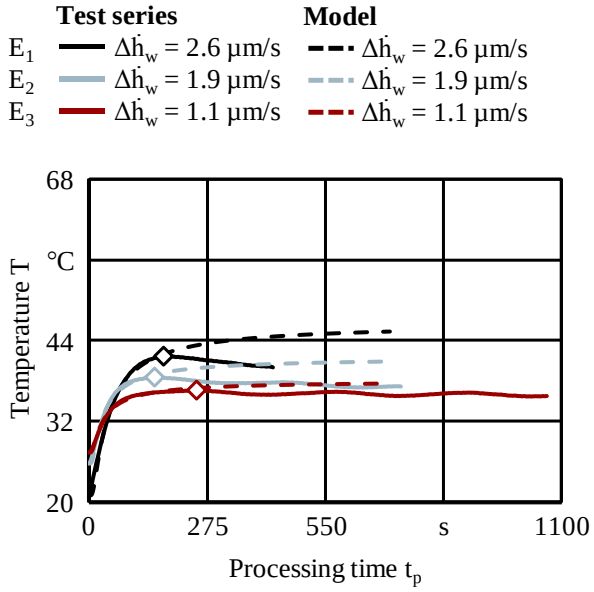

	Height of material removed during an experiment Δh_w	Processing time t_p	Time used for modelling t_m	Height of material removed Δh_w during t_m	Average material removal rate $\Delta\dot{h}_w$ during t_m	Initial temperature and model coefficients		
						T_0	b_1	b_2
	µm	s	s	µm	µm/s	°C	°C	s
E_1	1000	428	174	457	2.6	21.01	25.58	34.22
E_2	1000	726	151	282	1.9	25.72	15.79	26.54
E_3	1000	1066	249	278	1.1	27.31	10.68	26.90

Figure 8: Experimental and theoretical temperature, process parameters and model coefficients for grinding of C45 carbon steel with cutting speed $\bar{v}_c$ = 5 m/s and lubricant flow rate $\dot{Q}_{lub}$ = 20 l/min

4. ANALYSIS OF EXPERIMENTAL RESULTS

In the first stage of machining, the workpiece temperature increased rapidly after the beginning of each experiment. In the next stage, the intensity of the temperature rise decreased before reaching its maximum value. After that, a trend showing an increasing behaviour towards a maximum value, started to decrease, as seen in Figure 8. It was the result of cooling along with gradual wear of the tool during grinding. Therefore, the relationship between the workpiece temperature and the processing time was approximated considering the shapes of the experimentally determined curves, according to DEJA ET AL. [35] and KORZYŃSKI [46], as formulated in Equation 7 and Equation 8. Here, T is the expected workpiece temperature, T_0 is the workpiece temperature at the beginning of the experiment and ΔT is the temperature change, all temperatures are in degrees Celsius.

$$T = T_0 + \Delta T \tag{7}$$

$$\Delta T = b_1 \cdot \exp(-b_2/t_p) \tag{8}$$

Processing time t_p is given in seconds and b_1 as well as b_2 are model coefficients determined on the basis of experimental data. Coefficient b_1 is a horizontal asymptote in the proposed nonlinear regression model of temperature changes. Similar to DEJA ET AL. [35], this coefficient can be assumed as the theoretical maximum temperature increase that could occur during double face grinding under given technological parameters and initial thermal conditions such as the workpiece T_0. The software package Matlab® by THE MATHWORKS, INC., Natick, Massachusetts, USA, was used to process the data, build an exponential model and conduct the curve fitting. The evaluated values of coefficients for the experiments at $\bar{v}_c$ = 5 m/s are tabulated in Figure 8. One of the advantages of the proposed model is that the theoretical maximum temperature increase is specified directly as an asymptotic b_1 coefficient of the mathematical function expressed by Equation 8. Given this, the maximum workpiece temperature can be calculated from Equation 8, where T_{max} is the maximum workpiece temperature and ΔT_{max} is the maximum temperature increase.

$$T_{max} = T_0 + \Delta T_{max} \tag{9}$$

Since ΔT_{max} corresponds to coefficient b_1, the maximum workpiece temperature can be estimated based on Equation 10, where b_1 is a coefficient of a model used in Equation 8 and given in degrees Celsius [°C].

$$T_{max} = T_0 + b_1 \tag{10}$$

Next series of experiments: E_4, E_5 and E_6, were conducted using doubled cutting speed $\bar{v}_c$ = 10 m/s and flow of coolant $\dot{Q}_{lub}$ = 40 l/min. This resulted in higher temperatures and shorter processing times t_p caused by higher removal rates $\Delta\dot{h}_w$ during the experiments: E_4, E_5, E_6 - Figure 9.

Process
Double face grinding with planetary kinematics

Machine tool
Stähli DLM 505 HS

Workpiece

Type	Test workpiece, cylindrical			
Material	C45			
Radius	r	=	17.5	mm

Process parameter

Allocation	B	=	11.53	%
Mean Cutting speed	$\bar{v}_c$	=	10	m/s
Coolant lubricant	Rhenus GP5			
Volume flow	$\dot{Q}_{lub}$	=	40	l/min
Temperature	T_{lub}	=	21.7	°C

Tool

Type	D64 C75			
Grain material	CBN			
Bonding type	Synthetic resin			
Grain size	d_g	=	D64	
Grain concentration	C	=	3.3	ct/cm³
Outer radius	r_o	=	265	mm
Inner radius	r_i	=	132.5	mm

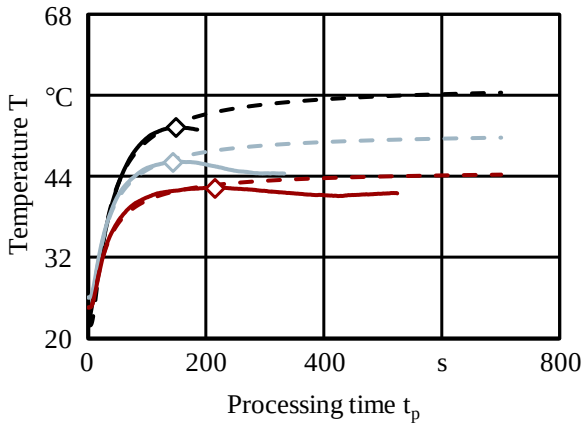

	Height of material removed during an experiment Δh_w	Processing time t_p	Time used for modelling t_m	Height of material removed Δh_w during t_m	Average material removal rate $\Delta\dot{h}_w$ during t_m	Initial temperature and model coefficients		
						T_0	b_1	b_2
	µm	s	s	µm	µm/s	°C	°C	s
E_4	1000	186	149	802	5.4	21.86	35.91	27.06
E_5	1000	333	143	528	3.7	26.05	24.59	26.12
E_6	1000	524	215	497	2.3	24.65	20.37	25.06

Figure 9: Experimental and theoretical temperature, process parameters and model coefficients for grinding of C45 carbon steel with cutting speed $\bar{v}_c$ = 10 m/s and lubricant flow rate $\dot{Q}_{lub}$ = 40 l/min

The first experiment E_4 was run with the material removal rate $\Delta\dot{h}_w$ = 5.4 μm/s. Due to the tool wear, the last experiment E_6 was run with the lowest material removal rate $\Delta\dot{h}_w$ = 2.3 μm/s. It was also slightly lower than the highest material removal rate $\Delta\dot{h}_w$ = 2.6 μm/s achieved in E_1 from the previous series, run with the lower coolant flow $\dot{Q}_{lub}$ = 20 l/min. Similar material removal rates from both series were reflected in minor differences between recorded and calculated temperatures, despite that the cooling intensity was doubled in the second series. Maximum temperatures recorded during experiments E_1 and E_6 were 41.68 °C and 42.28 °C, respectively. Maximum theoretical temperatures calculated for experiments E_1 and E_6, using Equation 10, are 46.6 °C and 45 °C, accordingly. The relatively small differences between measured and calculated temperature values from corresponding experiments E_1 and E_6 show that the influence of the coolant flow rate on the workpiece temperature was not as big as during machining of ceramic materials [35]. Most likely, it was the result of the thermal conductivity of steel materials, higher than that of ceramics. This allowed for efficient cooling of steel workpieces machined even at lower cooling intensity when $\dot{Q}_{lub}$ = 20 l/min.

Further increase in the cutting speed to $\bar{v}_c$ = 15 m/s, resulted in higher material removal rates $\Delta\dot{h}_w$ during the first two experiments of the third series: E_7 and E_8 – Figure 10. Similar behaviour was observed during the first two experiments of the second series: E_4 and E_5 – Figure 9. The maximum temperatures measured during E_7 and E_8 were 38.34 °C and 42.84 °C. They were lower than the maximum temperatures measured during E_4 and E_5, which were 51.26 °C and 46.11 °C.

Process
Double face grinding with planetary kinematics

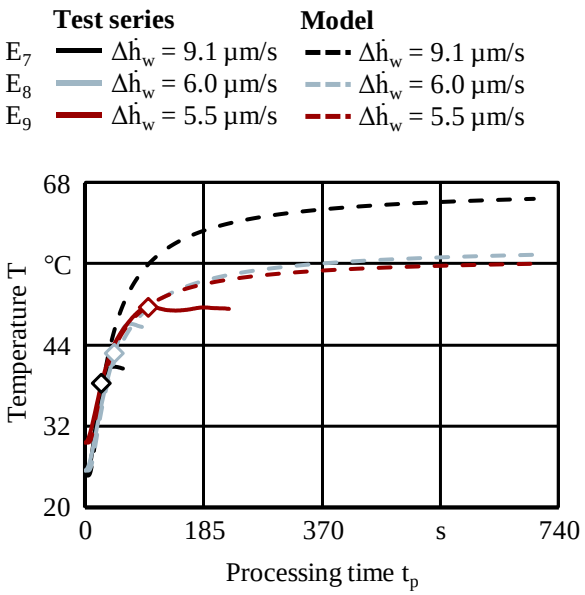

Machine tool
Stähli DLM 505 HS

Workpiece

Type	Test workpiece, cylindrical			
Material	C45			
Radius	r	=	17.5	mm

Process parameter

Allocation	B	=	11.53	%
Mean Cutting speed	$\bar{v}_c$	=	15	m/s
Coolant lubricant	Rhenus GP5			
Volume flow	$\dot{Q}_{lub}$	=	40	l/min
Temperature	T_{lub}	=	21.7	°C

Tool

Type	D64 C75			
Grain material	CBN			
Bonding type	Synthetic resin			
Grain size	d_g	=	D64	
Grain concentration	C	=	3.3	ct/cm³
Outer radius	r_o	=	265	mm
Inner radius	r_i	=	132.5	mm

	Height of material removed during an experiment Δh_w	Processing time t_p	Time used for modelling t_m	Height of material removed Δh_w during t_m	Average material removal rate $\Delta\dot{h}_w$ during t_m	Initial temperature and model coefficients		
						T_0	b_1	b_2
	µm	s	s	µm	µm/s	°C	°C	s
E_7	237	26	26	237	9.1	24.71	42.69	30.56
E_8	274	46	46	274	6.0	25.45	33.41	32.10
E_9	1000	225	99	541	5.5	29.52	27.63	30.30

Figure 10: Experimental and theoretical temperature, process parameters and model coefficients for grinding of C45 carbon steel with cutting speed $\bar{v}_c$ = 15 m/s and lubricant flow rate $\dot{Q}_{lub}$ = 40 l/min

Although the measured maximum temperatures were lower, the maximum temperatures calculated from the Equation 4, are higher: 67.4 °C for E_7 and 58.9 °C for E_8. The last experiment E_9 was run with the lowest material removal rate $\Delta\dot{h}_w$ = 5.5 µm/s which was slightly higher than the highest material removal rate $\Delta\dot{h}_w$ = 5.4 µm/s achieved in E_4 from the previous series, run with the same coolant flow $\dot{Q}_{lub}$ = 40 l/min but at lower cutting speed $\bar{v}_c$ = 10 m/s. Comparable material removal rates from both series again were reflected in close values of measured and calculated maximum temperatures depicted in Figure 11.

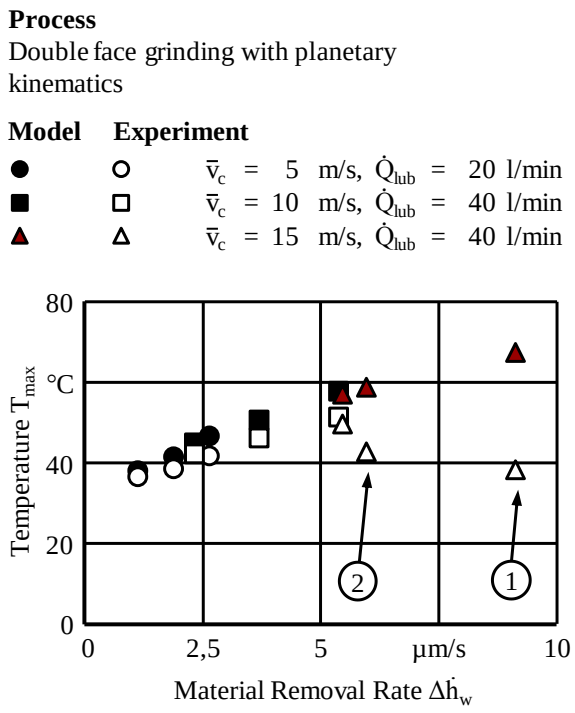

Figure 11: Experimental and theoretical maximum workpiece temperature

The trends in temperature rises anticipated on the basis of the theoretical analysis presented in Section 2 were observed during all performed grinding experiments. The wheel wear gradually reduced the grinding efficiency and measured temperature under unchanged technological process parameters and for the same mechanical properties of the work material and abrasive. Tool conditioning restored the abrasive properties which, in turn, caused that the workpiece temperature reached higher values again. The proposed empirical models can be used effectively in further research and in industrial practice due to accurate curve fitting and regarding the characteristics of an abrasive machining. In the production processes of mechanical components, finishing treatment by grinding requires usually shorter processing times due to the allowances smaller than 1 mm, as it was assumed in most of the conducted experiments apart from E_7 and E_8. In addition, the cutting ability of the grinding tools decreases with processing time. Lower cutting performance reduces the material removal rate $\Delta\dot{h}_w$ which leads to lower workpiece temperatures. Thus, the temperature should not exceed the theoretical maximum value T_{max} expressed by Equation 10, even for processes whose duration exceeds the time values used for modelling. Figure 11 shows the values of measured and calculated maximum temperatures for all experiments conducted with different cutting speeds. During subsequent experiments, the tool wear

caused a decrease in the material removal rate $\Delta\dot{h}_w$ which resulted in a longer processing time t_p and in lower workpiece temperatures. In addition, the measured temperatures were much lower than the calculated temperatures when the removal rate was high but the allowance for machining was smaller than $\Delta h_w = 1000$ μm, as occurred during E_7 ($\Delta h_w = 237$ μm) and E_8 ($\Delta h_w = 274$ μm) experiments – Figure 10 and Figure 11.

Obtained results showed that the workpiece temperature depends strongly on the grinding efficiency resulting from the actual state of the active surface of the grinding wheel, under constant technological parameters. Thus, the lower cutting speed may result in the higher workpiece temperature when an unworn tool is used (higher grinding performance), and accordingly, the lower temperature will be a result of the tool wear (lower grinding performance). The theoretical maximum workpiece temperatures presented in Figure 11 can be assumed as an upper boundary of the workpiece temperature rise that can occur during double face grinding in the analysed machining system, depending on the actual efficiency and regardless of the cutting speed.

5. CONCLUSIONS

The main advantages of double face grinding with planetary kinematics are increased efficiency, the tension-free workpiece clamping as well as evenly distributed load on the entire surface of the workpieces. The advantage of grinding over double face plane-lapping is also the lower environmental impact due to the substitution of the lapping emulsion containing loose grains by bonded grains in the grinding wheels and the use of a closed coolant circuit. As known from other grinding processes, the workpiece temperature has a considerable influence on the achievable surface quality, in particular the subsurface damage (SSD). To avoid grinding burns and thermally induced changes in the edge zone, the thermal analysis of this process is required as the achievable cutting speeds are much higher than in lapping. So far, the thermal characteristics of double face grinding have been studied only marginally compared to other grinding configurations, mainly due to the measurement difficulties in the machining system. The authors have developed a method for measuring the workpiece temperature in double face grinding with planetary kinematics and have successfully applied it for different materials, including difficult-to-cut ceramics. The influence of the mean cutting speed, the tool's cutting ability and the coolant flow rate on the temperature of C45 carbon steel workpieces have been investigated and reported in this paper. The main contribution and benefits of this work can be summarised as follows:

- Workpiece temperatures were measured during experiments carried out at three different cutting speeds and two cooling flow rates using full-featured digital temperature loggers. The lowest coolant flow rate $\dot{Q}_{lub}$ = 20 l/min was applied for the lowest average cutting speed $\bar{v}_c$ = 5 m/s. For higher speeds: $\bar{v}_c$ = 10 m/s and $\bar{v}_c$ = 15 m/s, more intensive cooling with the flow rate $\dot{Q}_{lub}$ = 40 l/min was used. Measurements of the workpieces temperature in the considered machining system have been reported in the literature only for Al_2O_3 ceramic materials.

- During subsequent experiments, the tool wear caused a decrease in the material removal rate $\Delta\dot{h}_w$ which resulted in a longer processing time t_p and lower workpiece temperatures T. Similar material removal rates during experiments conducted at different cutting speeds $\bar{v}_c$ were reflected in small differences between recorded and calculated temperatures.

- The empirical model to predict the temperature of C45 steel workpieces while processing was determined using the experimental results. It allows calculating the temperature increase as well as the maximum workpiece temperature under given technological parameters and initial thermal conditions such as the workpiece and lubricant temperatures.

- Experimental results showed that the influence of the coolant flow rate on the temperature of steel workpieces was not as big as during machining of ceramic materials [35]. Most likely, it was the result of the thermal conductivity of steel materials, which is higher than that of ceramics. This allowed for efficient cooling of steel workpieces machined even at lower cooling intensity.
- Proposed empirical models can be used effectively in further research and safely in industrial practice due to accurate curve fitting and regarding the characteristics of an abrasive machining. In the production processes of mechanical components, finishing treatment by grinding requires usually shorter processing times due to smaller allowances than in the experiments conducted. Smaller allowances will result in temperatures lower than maximum ones calculated from the determined models. It was confirmed during experiments carried out at the highest cutting speed $\bar{v}_c$ = 15 m/s.
- Further research will focus on the determination of the energy partition for double face grinding along with adopting the models based on the contact mechanics developed for lapping and superfinishing to estimate the temperature rises of the work surface.

ACKNOWLEDGEMENTS

Computations carried out with the use of software and computers from Academic Computer Centre in Gdańsk - TASK (http://www.task.gda.pl). Experiments were partially financed by Polish budget funds for science as a research project N N503 157638.

REFERENCES

[1] Funck, A. (1994). Planschleifen mit Läppkinematik. PhD-Thesis, Technische Universität Berlin.

[2] Ardelt, T. (2001). Einfluss der Relativbewegung auf den Prozess und das Arbeitsergebnis beim Planschleifen mit Planetenkinematik. PhD-Thesis, Technische Universität Berlin.

[3] Rußner, C. (2008). Präzisionsplanschleifen von Al_2O_3-Keramik unter Produktionsbedingungen. PhD-Thesis, Technische Universität Dresden.

[4] Uhlmann, E., List, M., Lichtschlag, L. (2016). Stellgrößen beim Doppelseitenplanschleifen mit Planetenkinematik. Zeitschrift für wirtschaftlichen Fabrikbetrieb ZwF, 111(7-8), 399 - 402.

[5] Uhlmann, E., List, M., Patraschkov, M., Trachta, G. (2018). A new process design for manufacturing sapphire wafers. Precision Engineering, 53, 146 - 150.

[6] Li, H. N., Yang, Y., Zhao, Y. J., Zhang, Z., Zhu, W., Wang, W., Qi, H. (2019). On the periodicity of fixed-abrasive planetary lapping based on a generic model. Journal of Manufacturing Processes, 44, 271-287.

[7] Wang, L., Hu, Z., Chen, Y., Yu, Y., Xu, X. (2019). Material removal mechanism of sapphire substrates with four crystal orientations by double-sided planetary grinding. Ceramics International, 46(6), 7813 - 7822.

[8] Uhlmann, E., Hoghé, T. (2012). Wear reduction at double face grinding with planetary kinematics. Production Engineering, 6(3), 237 - 242.

[9] Uhlmann, E., Hoghé, T., Kleinschnitker, M. (2013). Grinding wheel wear prediction at double face grinding with planetary kinematics using analytic simulation. The International Journal of Advanced Manufacturing Technology, 69(9-12), 2315 - 2321.

[10] Uhlmann, E., Kleinschnitker, M., Hoghé, T. (2014). Tool Wear model for double face grinding with planetary kinematics. In: Proceedings of the ASME 2014 International Manufacturing Science and Engineering Conference, Detroit, 09.06. - 13.06.2014.

[11] List, M. (2019). Ortsabhängiges Verschleißmodell für das Doppelseitenplanschleifen mit Planetenkinematik. PhD-Thesis, Technische Universität Berlin.

[12] Lichtschlag, L., List, M., Uhlmann, E. (2019). Entwicklung eines Systems zur Bestimmung des Profilverschleißes beim Doppelseitenplanschleifen mit Planetenkinematik. Ingenieurspiegel, 3, pp. 5 - 8.

[13] Lichtschlag, L., Uhlmann, E. (2019). Profilverschleißreduzierung beim Planschleifen. Werkstattstechnik online, 109(11-12), 847 - 851.

[14] Malkin, S., Guo, C. (2007). Thermal analysis of grinding. CIRP Annals, 56(2), 760-782.

[15] Moulik, P. N., Yang, H. T. Y., Chandrasekar, S. (2001). Simulation of thermal stresses due to grinding. International Journal of Mechanical Sciences, 43(3), 831-851.

[16] Kuang, W., Miao, Q., Ding, W., Zhao, Y., Zhao, Z. (2021). Residual stresses of turbine blade root produced by creep-feed profile grinding: Three-dimensional simulation based on workpiece–grain interaction and experimental verification. Journal of Manufacturing Processes, 62, 67-79.

[17] Jiang, J., Ge, P., Sun, S., Wang, D., Wang, Y., Yang, Y. (2016). From the microscopic interaction mechanism to the grinding temperature field: an integrated modelling on the grinding process. International Journal of Machine Tools and Manufacture, 110, 27-42.

[18] Zhu, B., Guo, C., Sunderland, J. E., Malkin, S. (1995). Energy partition to the workpiece for grinding of ceramics. CIRP annals, 44(1), 267-271.

[19] Kim, N. K., Guo, C., Malkon, S. (1997). Heat flux distribution and energy partition in creep-feed grinding. CIRP Annals, 46(1), 227-232.

[20] Guo, C., Wu, Y., Varghese, V., Malkin, S. (1999). Temperatures and energy partition for grinding with vitrified CBN wheels. CIRP Annals, 48(1), 247-250.

[21] Pang, J., Li, B., Liu, Y., Wu, C. (2016). Heat flux distribution model in the cylindrical grinding contact area. Procedia Manufacturing, 5, 158-169.

[22] Bulsara, V. H., Ahn, Y., Chandrasekar, S., Farris, T. N. (1997). Polishing and lapping temperatures. Journal of Tribology, 119(1), 163-170.

[23] Jaeger J. C. (1942). Moving sources of heat and the temperature at sliding contacts. Proceedings of the Royal Society of New South Wales, 76, 203-224.

[24] Blok, H. (1937). Theoretical study of temperature rise at surface of actual contact under oiliness lubricating conditions. Proceedings of the General Discussion on Lubrication & Lubricants, Vol. 2, The Institution of Mechanical Engineers, 222-235.

[25] Horng, J. H., Jeng, Y. R., Chen, C. L. (2004). A model for temperature rise of polishing process considering effects of polishing pad and abrasive. Journal of Tribology, 126(3), 422-429.

[26] Chen, Y., Zhang, L. C., Arsecularatne, J. A., Montross, C. (2006). Polishing of polycrystalline diamond by the technique of dynamic friction, part 1: Prediction of the interface temperature rise. International Journal of Machine Tools and Manufacture, 46(6), 580-587.

[27] Wu, H. W., Chen, Y. Y., Horng, J. H. (2017). The analysis of three-body contact temperature under the different third particle size, density, and value of friction. Micromachines, 8(10), 302.

[28] Nayak, B., Babu, N. R. (2020). Influence of tool and workpiece interface temperature rise on the life of ice bonded abrasive polishing tool. Wear, 462, 203511.

[29] Chang, S. H., Farris, T. N., Chandrasekar, S. (2000). Contact mechanics of superfinishing. Journal of Tribology, 122(2), 388-393.

[30] Brinksmeier, E., Aurich, J. C., Govekar, E., Heinzel, C., Hoffmeister, H. W., Klocke, F., Peters J., Rentsch R., Stephenson D. J., Uhlmann E., Weinert, K. (2006). Advances in modeling and simulation of grinding processes. CIRP annals, 55(2), 667-696.

[31] Deja, M., Zieliński, D. (2020). Wear of electroplated diamond tools in lap-grinding of Al_2O_3 ceramic materials. Wear, 460, 203461.

[32] Agarwal, S. (2019). On the mechanism and mechanics of wheel loading in grinding. Journal of Manufacturing Processes, 41, 36-47.

[33] Rowe, W. B. (2013). Principles of Modern Grinding Technology. Boston: Elsevier.

[34] Marinescu, I. D., Hitchiner, M. P., Uhlmann, E., Rowe, W. B., Inasaki, I. (2016). Handbook of Machining with Grinding Wheels. Boca Raton: CRC Press.

[35] Deja, M., List, M., Lichtschlag, L., Uhlmann, E. (2019). Thermal and technological aspects of double face grinding of Al_2O_3 ceramic material. Ceramics International, 45(15), 19489 - 19495.

[36] Oliveira, J. F. G., Silva, E. J., Guo, C., Hashimoto, F. (2009). Industrial challenges in grinding. Annals of the CIRP 58(2), 663 - 680.

[37] Barylski, A., Deja, M. (2010). Wear of a Tool in Double-Disk Lapping of Silicon Wafers. Proceedings of the ASME 2010 International Manufacturing Science and Engineering Conference. ASME 2010 International Manufacturing Science and Engineering Conference, Volume 1. Erie, Pennsylvania, USA. October 12–15, 2010. pp. 301-307. ASME. https://doi.org/10.1115/MSEC2010-34323 .

[38] Deja, M. (2010). Simulation Model for the Shape Error Estimation During Machining With Flat Lapping Kinematics. Proceedings of the ASME 2010 International Manufacturing Science and Engineering Conference. ASME 2010 International Manufacturing Science and Engineering Conference, Volume 1. Erie, Pennsylvania, USA. October 12–15, 2010. pp. 291-299. ASME. https://doi.org/10.1115/MSEC2010-34262.

[39] Barylski, A., Piotrowski, N. (2019). Non-conventional approach in single-sided lapping process: kinematic analysis and parameters optimization. The International Journal of Advanced Manufacturing Technology, 100(1-4), 589-598.

[40] Piotrowski, N. (2020). Tool Wear Prediction in Single-Sided Lapping Process. Machines, 8(4), 59.

[41] Lai, Z., Hu, Z., Fang, C., Yu, Y., Hsieh, P., Chen, M. (2020). Research on factors affecting wear uniformity of the wheels in the double-sided lapping. Journal of Manufacturing Processes, 50, 653-662.

[42] Deja, M. (2012). Correlation between shape errors in flat grinding. Journal of Vibroengineering, 14(2), 520 - 527.

[43] Maxim Integrated Products, Inc. "DS1922L iButton Temperature Loggers with 8KB Data-Log Memory" San Jose, CA, United States. URL: https://www.maximintegrated.com/en/products/ibutton-one-wire/data-loggers/DS1922L.html (access: 2021-01-02).

[44] Maxim Integrated Products, Inc. ”DS1922E iButton High-Temperature Logger with 8KB Data-Log Memory.” San Jose, CA, United States. URL: https://www.maximintegrated.com/en/products/ibutton-one-wire/data-loggers/DS1922E.html (access: 2021-01-02).

[45] Sampurno, Y. A., Borucki, L., Zhuang, Y., Boning, D., Philipossian, A. (2005). A method for direct measurement of substrate temperature during copper CMP. Journal of the Electrochemical society, 152(7), G537.

[46] Korzyński M. (2018). Methodology of the experiment. Planning, implementation and statistical analysis of the results of technological experiments”, in Polish “Metodyka eksperymentu. Planowanie, realizacja i statystyczne opracowanie wyników eksperymentów technologicznych”, Publisher House: Wydawnictwo WNT.